STAT3 Inhibits Cell Proliferation at Least in Part Via Directly Negatively Regulating FST Gene Expression

Haidong Xu
Northeast Agricultural University
Guangwei Ma
Hainan Normal University
Fang Mu
Northeast Agricultural University
Bolin Ning
Northeast Agricultural University
Hui Li
Northeast Agricultural University
Ning Wang (wangning@neau.edu.cn)
Northeast Agricultural University

Research

Keywords: STAT3, FST, transcriptional regulation, cell proliferation, sheep

Posted Date: January 6th, 2021

DOI: https://doi.org/10.21203/rs.3.rs-139647/v1

STAT3 inhibits cell proliferation at least in part via directly negatively regulating *FST* gene expression

Running Title: *FST* is a target gene of STAT3

Haidong Xu[1†], Guangwei Ma[1,2†], Fang Mu[1], Bolin Ning[1], Hui Li[1], Ning Wang[1*]

[1] Key Laboratory of Chicken Genetics and Breeding, Ministry of Agriculture and Rural Affairs & Key Laboratory of Animal Genetics, Breeding and Reproduction, Education Department of Heilongjiang Province & College of Animal Science and Technology, Northeast Agricultural University, Harbin 150030, China.

[2] Ministry of Education Key Laboratory for Ecology of Tropical Islands & Key Laboratory of Tropical Animal and Plant Ecology of Hainan Province & College of Life Sciences, Hainan Normal University, Haikou 571158, China.

* Correspondence: wangning@neau.edu.cn

† Haidong Xu and Guangwei Ma contributed equally to this work.

Abstract

Background: Follistatin (FST) is a secretory glycoprotein and belongs to the TGF-β superfamily. Previously, we found that two single nucleotide polymorphisms (SNPs) of sheep *FST* gene were significantly associated with wool quality traits in Chinese Merino sheep (Junken type), indicating that FST is involved in the regulation of hair follicle development and hair trait formation. The transcription regulation of human and mouse *FST* genes has been widely investigated, and many transcription factors have been identified to regulate *FST* gene, such as erythroid 2-related factor 2 (Nrf2), Estrogen-related receptor-β (ERRβ), β-catenin/transcription factor 4 (TCF4) and transcription factor Sp1. However, to date, the transcriptional regulation of sheep *FST* is largely unknown. The objective of this study was to investigate the transcriptional regulation of sheep *FST* gene in hair follicles.

Results: Genome walking analysis revealed that the gap region upstream of sheep genomic *FST* gene was 775 bp long. Transcription factor binding site analysis showed sheep *FST* promoter region contained a conserved putative binding site for signal transducer and activator of transcription 3 (STAT3), located at nucleotides -423 to -416 relative to the first nucleotide (A, +1) of the initiation codon (ATG). The dual-luciferase reporter assays showed that STAT3 inhibited the activity of the *FST* promoter reporter, and the mutation of the putative STAT3 binding site attenuated the inhibitory effect of STAT3 on the *FST* promoter activity. Furthermore, chromatin immunoprecipitation assay (ChIP) indicated that STAT3 directly binds to the *FST* promoter. The further functional study displayed that *FST* and *STAT3* played opposite roles in cell proliferation. Overexpression of *FST* significantly promoted the proliferation of sheep fetal fibroblasts (SFFs) and human keratinocyte (HaCaT) cells, and overexpression of *STAT3* significantly inhibited the proliferation of SFFs and HaCaT cells, which was accompanied by a significantly reduced expression of *FST* gene ($P < 0.05$).

Conclusions: STAT3 directly negatively regulates sheep *FST* gene and inhibits cell proliferation. The findings will contribute to understanding molecular mechanisms that underlie hair follicle development and wool trait formation.

Keywords: STAT3, *FST*, transcriptional regulation, cell proliferation, sheep

Background

Wool is the product of hair follicles and wool traits are influenced by hair follicles. The hair follicle is a skin appendage with a complex structure composed of the dermal papilla, hair bulbs, outer root sheaths (ORS), inner root sheaths (IRS), and the hair matrix [1, 2]. Hair follicle morphogenesis and development involve proliferation, differentiation and apoptosis of hair follicle stem cells [2, 3]. The hair follicle undergoes life-long cyclic transformations exhibiting anagen (growth), catagen (regression), and telogen (rest) phases, respectively [1, 4]. A variety of growth factors and cytokines have been shown to tightly regulate the hair follicles morphogenesis and development through acting on the epithelial-mesenchymal interaction [5, 6], such as fibroblast growth factor (FGF) [7], tumor necrosis factor (TNF) [8] and transforming growth factor-β (TGF-β) [9]. As an antagonist of the TGF-β superfamily, follistatin (FST) is highly expressed in the matrix of hair follicles which consist of cells with a strong proliferation ability [10]. *FST* transgenic mice exhibited shinier and more irregular hair [11, 12]. *FST* knockout mice died within hours after birth and displayed curlier whiskers [13-15]. Our previous association analysis demonstrated that *FST* gene was significantly associated with wool quality traits in Chinese Merino sheep (Junken Type) [10]. Collectively, these data indicated that FST is involved in the regulation of hair follicle development and hair trait formation.

The transcriptional regulation of human and mouse *FST* genes has been widely investigated, and many transcription factors have been identified to regulate *FST* gene. For example, Nrf2 directly regulates *FST* gene and inhibits the apoptosis of human lung epithelial cells and A549 cells [16]. TCF4 complex directly regulates *FST* gene and promotes the myogenic differentiation and myoblast fusion *in vitro* [17]. MyoD and Sox8 suppress *FST* gene expression in skeletal muscle myoblast cells *in vitro* [18]. Myogenin directly regulates *FST* gene and promotes the satellite cell differentiation in adult mouse myogenesis [19]. ERRβ directly promotes *FST* expression to inhibit epithelial to mesenchymal transition in breast cancer [20]. SP1 directly promotes *FST* expression in intestinal epithelial cells and kidney mesangial cells [21, 22]. However, to date, the transcriptional regulation of sheep *FST* is largely unknown.

STAT3 is an important transcriptional factor that regulates follicle morphogenesis and development. It is vital for maintaining keratinocyte stem/progenitor cell homeostasis via facilitating the maturation of bulge region in mouse hair follicle development [23-26]. However, it

is unknown whether STAT3 directly regulates *FST* gene. In the present study, our results demonstrated that STAT3 directly negatively regulates *FST* gene and inhibits the proliferation of SFFs and HaCaT cells.

Methods

Ethics statement

All animal works were conducted according to the guidance for the care and use of experimental animals established by the Ministry of Science and Technology of the People's Republic of China (Approval number: 2006-398) and approved by the Laboratory Animal Management Committee of Northeast Agricultural University.

Cell culture

HEK293 and HaCaT cells were purchased from the China Center for Type Culture Collection, and cultured in Dulbecco's Modified Eagle's Medium (DMEM) (Gibco, United States). SFFs as a kind gift from Dr. Tie-Zhu An, Northeast Forestry University, Harbin, were grown in DMEM-F12 (Gibco, United States). Both DMEM and DMEM-F12 were supplemented with 10% fetal bovine serum (FBS) (Biological Industries, Germany) and 1% penicillin/streptomycin (Gibco, United States). All cells were cultured in a humid environment with 5% CO_2 in the air at 37℃.

Closing gap upstream of sheep *FST* gene

Genomic DNA was isolated from sheep skin samples, previously collected and preserved [10], using the phenol-chloroform method [27] and stored at -20℃. There is a gap upstream of sheep *FST* gene according to Ovis aries reference genome (ISGC Oar_v3.1/oviAri3), which locates on chr16 (position: 25,635,265-25,636,038 bp). To close this gap, we performed genome walking according to the manufacturer's instructions [28]. Briefly, three specific reverse primers: FST-SP1, FST-SP2, and FST-SP3 (Table 1), were designed, and their locations are shown in Supplement Figure 1. Three forward primers, ZFP2, ZSP1 and ZSP2 were provided by the KX Genome Walking Kit (Zoman Biotechnology, China). Three rounds of nested PCR were performed with these primers. The primers ZFP2 and FST-SP1 were used to conduct the first-round PCR, the primer pairs ZSP1/FST-SP2 and ZSP2/FST-SP3 were used to conduct the second-and third-round PCRs. The first-round PCR was performed in a total volume of 50 μL containing 200 ng genomic DNA, 2.5 mM dNTPs, 25 μL of 2×Kx PCR Buffer (with Mg^{2+}), 1U / μL Kx Pfu DNA Polymerase,

and 10 pmol/μL primers (ZFP2 and FST-SP1). The PCR conditions were as follows: initial denaturation at 94℃ for 2 min, followed by 2 cycles (98℃ for 10 s, 60℃ for 30 s, 68℃ for 2 min), 98℃ for 10 s, 25℃ for 2 min, 25 to 68℃ for 0.2℃/s, 68℃ for 2 min, 6 cycles (98℃ for 10 s, 60℃ for 30 s, 68℃ for 2 min, 98℃ for 10 s, 60℃ for 30 s, 68℃ for 2 min, 98℃ for 10 s, 44℃ for 30 s, 68℃ for 2 min), with a final extension at 68℃ for 5 min. The first-round PCR amplification products (1 μL) were used as templates for the second-round PCR and the other PCR components were the same as the first-round PCR, and run at thermal protocol for 94℃ for 2 min, followed by 30 cycles (98℃ for 10 s, 60℃ for 30 s, 68℃ for 2 min), with a final extension at 68℃ for 5 min. The second-round PCR products (1 μL) were used as templates for the third-round PCR and the other PCR components were the same as those used in the second round PCR, and a total of 12 cycles were performed the third-round PCR. The third-round PCR products were resolved on a 1.2% agarose gel, recovered and cloned into pEASY-T1 Simple Cloning Vector (TransGen Biotech, China). The recombinant plasmids were sequenced in both directions to confirm the authenticity of the sequences.

Bioinformatics analysis

In this study, the first nucleotide (A) of the initiation codon (ATG) of *FST* was assigned position +1. The *FST* promoter sequences of different animal species were obtained from the UCSC website (http://genome.ucsc.edu/). The conserved transcription factor binding sites were predicted by using Mulan website tool (https://mulan.dcode.org/) [29].

Plasmid construction

For the construction of *FST* and *STAT3* expression vectors, based on *FST* (NM_001257093.1) and *STAT3* (XM_015098787) mRNA sequences, two pairs of primers (FST-P1 and STAT3-P1, Table 1) were designed to amplify the full-length coding regions (CDSs) of sheep *FST* and *STAT3* gene. The full-length CDSs of *FST* and *STAT3* were amplified by RT-PCR from the pooled total RNA of sheep side skin tissues (n=3), using the primers FST-P1 and STAT3-P1, respectively. Both the RT-PCR products were individually cloned into the pCMV-Myc vector (Clontech, United States), and named pCMV-Myc-FST and pCMV-Myc-STAT3, respectively.

For the construction of *FST* promoter luciferase reporter vectors, sheep *FST* gene promoter fragment with the contained conserved putative STAT3 binding site, which was located between the -980 and -340 bp upstream of the initiation codon (ATG) of sheep *FST* gene, was amplified in

opposite directions with two pairs of primers FST-P3 and FST-P4 (Table 1) using the sheep genomic DNA as the template. Subsequently, the amplified *FST* promoter fragments were inserted into the *Kpn* I and *Hind* III site of pGL3-basic (Promega, United States) to yield two *FST* promoter reporters. The reporter with the *FST* promoter fragment in the right direction was named pFST (-980/-340) and the other one with the *FST* promoter fragment in opposite direction was named pFST (-340/-980). The putative STAT3 binding site was mutated from CGA*TTCC*CC to CGA*GGTA*CC in the reporter pFST(-980/-340) using the Fast Mutagenesis System (TransGen Biotech, China) and FST-P5 primers according to the manufacturer's recommendation. The resultant reporter construct was named pFST(-980/-340)-mutSTAT3. All primers were synthesized by Invitrogen (Shanghai, China) and all constructs were confirmed by DNA sequencing (Invitrogen, Shanghai, China).

Transfection and dual-luciferase report assay

Briefly, the HEK293 cells were seeded in a 24-well plate (2×10^5 cells / well) and cultured in the DMEM medium supplemented with 10% FBS and 1% penicillin/streptomycin. After reaching 70-80% confluence, the cells were washed with phosphate buffer saline (PBS) and transient transfection was performed using Lipofectamine 2000 (Invitrogen, United States). Dual-luciferase reporter assays were performed 48 h post-transfection using the dual-luciferase reporter assay system (Promega, United States) according to the manufacturer's instructions. The Firefly luciferase (*Fluc*) activity was normalized to Renilla luciferase (*Rluc*) activity.

Western blot analysis

Cultured cells were washed three times with cold PBS and lysed in 6-well plates by using 100 μL RIPA Buffer (Beyotime Biotechnology, China) containing 1 μL phenyl methane sulfonyl fluoride (Beyotime Biotechnology, China). After incubation on ice for 30 min, the supernatant was collected by centrifugation at 10, 000 × g for 5 min at 4℃. The equal amounts of protein from the cell lysates were separated by 12% SDS-polyacrylamide gel electrophoresis and transferred to nitrocellulose membranes (Millipore, United States). The blots were blocked in PBS containing 5% (w/v) dry milk and 0.1% Tween 20 for 2 h and then incubated with primary antibody dilution buffer (Beyotime Biotechnology, China) containing Myc-tag mouse monoclonal antibody (Abcam, 1:1,000) at room temperature for 2 h. After washing with PBS three times, the blots were incubated with a secondary antibody dilution buffer containing horseradish peroxidase-conjugated

anti-mouse secondary antibody (Abcam, 1:5,000) for 1 h, followed by washing three times with PBS. The blots were visualized using an ECL Plus detection kit (Beyotime Biotechnology, China).

CCK-8 assay

The Cell Counting Kit-8 (CCK-8) assay was used to assay cell proliferation. Briefly, the SFFs and HaCaT cells were seeded in a 96-well plate (2×10^4 cells / well) and cultured in the DMEM-F12 and DMEM medium, respectively, supplemented with 10% FBS and 1% penicillin/streptomycin. At 12 h after seeding, transient transfections were performed using Lipofectamine 2000 (Invitrogen, United States). At 24, 48, and 72 h after transfection, each well was added with 10 μL CCK-8 solution (TransGen Biotech, China) and incubated at 37℃ for 2 h, and then the absorbance was recorded at 450 nm using a Model 680 Microplate Reader (Bio-Rad, United States).

Chromatin immunoprecipitation (ChIP) assay

Chromatin immunoprecipitation was performed using a ChIP assay kit (Beyotime Biotechnology, China) as previously described [30]. HEK293 cells were co-transfected with pFST(-980/-340) and pCMV-Myc-STAT3 or an empty pCMV-Myc vector. At 48 h post-transfection, the transfected cells were fixed with 1% formaldehyde at room temperature for 10 min. The Chromatin was digested with 0.5 μL micrococcal nuclease into 100–900 bp DNA/protein fragments, and immunoprecipitated using with 5 μg of Myc-specific antibody (Abcam, United States) and mouse IgG (Beyotime Biotechnology, China), respectively. The purified DNA fragments were analyzed by quantitative PCR using the primers FST-P6 (Table 1), which was performed on the 7500 Fast Real-Time PCR System (Applied Biosystems, United States) with SYBR Green PCR Master Mix (Roche Molecular Systems, United States). Non-immunoprecipitated DNA (2%) was used as input control. The qPCR data were normalized to input chromatin DNA and presented as fold enrichment over the negative control using ΔCt equation [31], which signal relative to input $=0.2 \times 2^{-\Delta Ct}$, $\Delta Ct=Ct_{[IP\ sample]} - Ct_{[Input\ sample]}$ [32].

RNA isolation and quantitative real-time PCR

Total RNA was isolated from the cultured cells using Trizol reagent (Invitrogen, United States) according to the standard procedures, and RNA quality was assessed by denaturing formaldehyde agarose gel electrophoresis. Reverse transcription was performed with ImProm-II Reverse Transcriptase (Promega, United States) according to the manufacturer's protocols. Quantitative

real-time PCR was carried out in a 7500 Fast Real-Time PCR System (Applied Biosystems, United States) with the SYBR Green PCR Master Mix (Roche Molecular Systems, United States). The primers used for qRT-PCR are listed in Table 1. Thermal cycling consisted of an initial step at 95℃ for 10 min followed by 40 cycles at 95℃ for 30 s and 60℃ for 30 s. The target gene expression was normalized to the *GAPDH* gene using the $2^{-\Delta Ct}$ method, where $\Delta Ct = Ct_{[target]}$ gene$-Ct_{[GAPDH]}$.

Statistical analysis

Data were expressed as the mean ± SE and analyzed with SAS 9.1.3 (SAS Institute Inc., NC). The student's *t*-test was used to examine the significance of the difference in gene expression. Statistical significance was indicated by $*P < 0.05$, $**P < 0.01$.

Results

Sheep *FST* promoter contains a conserved STAT3 binding site

There is a genomic gap immediate upstream of sheep *FST* gene according to the reference genome (ISGC Oar_v3.1/oviAri3), which locates on chr16 (positions: 25,635,263-25,636,038 bp). To obtain the promoter sequence of sheep *FST* gene, we first closed the genomic gap by genome walking. The results showed that the gap sequence was 775 bp in length and submitted to GenBank (Accession No. MT917184). Then we filled the gap and obtained the 3 kb genomic sequences immediate upstream of the initiation codon (ATG) of sheep *FST* genes from the UCSC website (http://genome.ucsc.edu/). The 3 kb genomic sequences of various animal species were also obtained from the UCSC website (http://genome.ucsc.edu/), including sheep, cow, pig, human, mouse, and rat. Using the Mulan website tool (https://mulan.dcode.org/) [29], many conserved putative binding sites of transcription factors were predicted within the -1,900/-1 region of the sheep *FST* gene, such as homeobox A4 (HOXA4), E2F transcription factor 2 (E2F2), hepatocyte nuclear factor 4 (HNF4), and STAT3. Of these transcription factors, STAT3 interested us. As shown in Figure 1A, the putative STAT3 binding sites were conserved among various species. STAT3 has been well defined as a key transcription factor for cell signal activation and transduction and plays critical roles in various biological activities including cell proliferation, migration, survival and oncogenesis [23, 33]. Furthermore, several independent lines of evidence

indicated that STAT3 is implicated in hair follicle morphogenesis and development [34, 35]. These data led us to speculate that STAT3 may directly regulate *FST* gene in hair follicle development.

STAT3 inhibits the *FST* promoter activity

To test the speculation whether STAT3 directly regulates *FST* gene expression, firstly, we constructed and verified the STAT3 expression vector, pCMV-Myc-STAT3 by western blotting (Figure 1B). A highly conserved region (-980/-340) of sheep *FST* promoter, which contained the putative conserved STAT3 binding site, was amplified and cloned into pGL3-basic vector in opposite direction, respectively, yielding the *FST* promoter reporters: pFST(980/-340) and pFST(-340/-980) as a negative control. In addition, the *FST* promoter reporter with mutation of the STAT3 binding site, named pFST(-980/-340)-mutSTAT3, was constructed. The reporter gene assay showed that, as expected, both pGL3-basic vector and pFST(-340/-980) as a negative control had very lower luciferase activity, and no difference in luciferase activity was observed between them ($P > 0.05$, Figure 1C). The luciferase activity of pFST(-980/-340) and pFST(-980/-340)-mutSTAT3 plasmids were 3.39- and 6.23-fold higher than that of the pGL3-basic vector ($P < 0.05$, Figure 1C), suggesting that the -980/-340 *FST* promoter region has promoter activity and that mutation of STAT3 binding site increases the promoter activity of *FST* gene.

Co-transfection analysis showed that the luciferase activity of pFST(-980/-340) was significantly reduced by 22.83% in the cells co-transfected with pCMV-Myc-STAT3, as compared with the cells co-transfected with pCMV-Myc ($P < 0.05$, Figure 1D). Intriguingly, the luciferase activity of pFST(-980/-340)-mutSTAT3 was also significantly reduced in the cell co-transfected with pCMV-Myc-STAT3, as compared with the cells co-transfected with pCMV-Myc ($P < 0.05$, Figure 1D). Taken together, these data suggested that STAT3 inhibits sheep *FST* promoter activity.

Furthermore, to investigate whether STAT3 directly binds to and regulates *FST* promoter, the pFST(-980/-340) and pCMV-Myc-STAT3 were co-transfected into HEK293 cells, and chromatin immunoprecipitation (ChIP) assay was employed with a Myc-specific antibody or mouse IgG (negative control). Two additional negative controls (A and B) were prepared by the co-transfection of HEK293 cells with pFST(-980/-340) and empty pCMV-Myc vector, and immunoprecipitation with either mouse IgG (A) or Myc-specific antibody (B). The ChIP-qPCR results showed that the *FST* promoter fragment (-547/-356) was significantly enriched (6.16, 20.55, 8.89-fold, respectively) in the DNA immunoprecipitated by the Myc-specific antibody compared

with the negative controls (mouse IgG, A and B) ($P < 0.05$, Figure 1E). Consistent with the ChIP-qPCR results, agarose gel electrophoresis showed that, compared with the negative control (mouse IgG, A, and B), more PCR products (-547/-356 region of *FST* promoter) were obtained from the DNA fragments immunoprecipitated by the Myc-specific antibody (Figure 1F). In summary, these data indicated that STAT3 directly binds to and regulates the *FST* promoter.

STAT3 and FST have opposite effects on cell proliferation

Previous studies demonstrated that *FST* overexpression promoted satellite cell proliferation and stimulated muscle fiber hypertrophy in mice [36] and duck [37]. In contrast, several studies showed *STAT3* overexpression inhibited the proliferation of leukocytes [38], hepatocytes [39], and chondrogenic cell line ATDC5 [40]. These data suggest that both FST and STAT3 play opposite roles in cell proliferation. To test whether *FST* mediates the roles of STAT3 in cell proliferation, we constructed and confirmed the *FST* expression vector (pCMV-Myc-FST) by western blotting (Figure 2A), and investigated the effects of overexpression of *STAT3* and *FST* on cell proliferation using the CCK-8 assay. The results showed that the absorbance of both the SFFs and HaCaT cells transfected with pCMV-Myc-FST was significantly higher than that of the cells transfected with the empty vector pCMV-Myc at 96 h of transfection ($P < 0.01$, Figure 2B and C), suggesting that FST promotes the proliferation of SFFs and HaCaT cells. The absorbance of both the SFFs and HaCaT cells transfected with pCMV-Myc-STAT3 was significantly lower than those of the cells transfected with the empty vector pCMV-Myc at 48 h and 72 h of transfection ($P < 0.01$, Figure 3A and B), suggesting that STAT3 inhibits the proliferation of SFFs and HaCaT cells. In parallel, we detected the expression of proliferation marker genes, *Ki67* and proliferating cell nuclear antigen (*PCNA*), using qRT-PCR. Consistent with CCK-8 assay results, *FST* overexpression significantly promoted *Ki67* and *PCNA* expression in the SFFs ($P < 0.05$, Figure 2D and E), while *STAT3* overexpression significantly inhibited *Ki67* and *PCNA* expression in the SFFs, compared with the empty vector pCMV-Myc at 48h of transfection ($P < 0.05$, Figure 3C and D). Further gene expression analysis showed *STAT3* overexpression significantly reduced the endogenous *FST* expression in both SFFs and HaCaT cells by 76.39% and 71.36%, respectively, compared with the empty vector pCMV-Myc at 48 h of transfection ($P < 0.05$, Figure 3E and F).

Taken together, these data not only support that STAT3 negatively regulates *FST* gene expression, but also indicate that STAT3 inhibits cell proliferation at least in part via directly downregulating *FST* gene expression.

Discussion

In the present study, we demonstrated that STAT3 directly negatively regulates sheep *FST* gene. Our evidences are as follows: (1) Bioinformatics analysis showed that *FST* promoter harbored a conserved putative STAT3 binding site (Figure 1A). (2) The luciferase reporter assay showed that mutation of STAT3 binding site led to an increase in the *FST* promoter activity and that STAT3 inhibited the *FST* promoter activity (Figure 1C and D). (3) The ChIP-qPCR assay showed that STAT3 directly bound to the *FST* promoter (Figure 1E and F). (4) Further functional analysis showed that *FST* and *STAT3* overexpression had opposite effects on the proliferation of SFFs and HaCaT cells (Figure 2 and 3) and that STAT3 overexpression inhibited the endogenous FST expression in SFFs and HaCaT cells (Figure 3E and F). Many target genes of STAT3 have been identified, such as forkhead box L2 (FOXL2) [41] and interleukin 17A (IL-17A) [42] interferon regulatory factor (IRF-4) and Bcl-6 [43]. To our knowledge, in the present study, we for the first time demonstrated that *FST* is a bona fide target gene of STAT3 and that STAT3 directly negatively regulates the *FST* gene and inhibits cell proliferation.

STAT3 belongs to the signal transduction and transcription activation factor family and is an important transcription factor for cell signal activation and transduction [44]. In the present study, we found that the STAT3 negatively regulated *FST* gene and inhibited cell proliferation (Figures 1, 2 and 3). Considering that transcription factors have multiple target genes, we cannot exclude the possibility that STAT3 inhibits cell proliferation in part by directly and/or indirectly regulating the expression of other target genes. Interestingly, a partial inhibitory effect of STAT3 on the promoter activity of pFST(-980/-340)-mutSTAT3 was observed, as compared with the cells co-transfected with pCMV-Myc ($P < 0.05$, Figure 1D). This may be dual to several reasons. Firstly, STAT3 may bind to its noncanonical binding sites in this *FST* promoter and inhibit *FST* promoter activity. Secondly, STAT3 may indirectly regulate *FST* promoter activity through regulation of the expression of the transcription factors which have binding sites in *FST* promoter. Lastly, STAT3 may indirectly regulate *FST* promoter activity by protein interaction with some transcription

306 factors, which have binding sites in *FST* promoter. Further study is required to determine the
307 precise mechanism underlying the partial inhibitory effect of STAT3 on the reporter
308 pFST(-980/-340)-mutSTAT3 in the future.
309 In the present study, we demonstrated that sheep *FST* overexpression promoted SFFs and HaCaT
310 cell proliferation (Figure 2B-E). In agreement with our results, it has been shown that FST
311 promotes the proliferation of duck primary myoblasts [45]. The knock-down of *FST* significantly
312 reduced the proliferation of the immortalized ovarian surface epithelial and human ovarian
313 carcinoma cell line SKOV3 [46]. Previous studies showed *STAT3* overexpression inhibited the
314 proliferation of mouse leukocyte and hepatocyte via inhibiting *cyclin D* expression [38, 39], as
315 well as chondrogenic cell line ATDC5 [40]. In agreement, our results showed that *STAT3*
316 overexpression inhibited the proliferation of SFFs and HaCaT cells (Figure 3A-D). However, it
317 has been shown that *STAT3* overexpression has been shown to promote human breast cancer [47,
318 48] and thyroid carcinoma [44] cell proliferation. These differences suggest that STAT3 may play
319 different roles in cell proliferation, depending on cell type, cellular context, and species.
320 Our results demonstrated that STAT3 negatively regulated the *FST* gene in SFFs and HaCaT cells.
321 SFFs are a type of mesenchymal cells [49, 50], and HaCaT cells, a spontaneously immortalized,
322 human keratinocyte line, represent epithelial cells [51, 52]. Therefore, SFFs and HaCaT cells
323 could partially represent hair follicle cells. Previous studies have demonstrated that STAT3 and
324 FST function in hair follicle development and cycles. STAT3 activation was a prerequisite for the
325 early anagen of hair follicles [23] and that keratinocytes-specific STAT3 knockout mice exhibited
326 impaired hair cycle [35]. FST promotes hair follicle development via binding activins and
327 preventing the activation of activin receptors [53]. FST knockout mice displayed thin and curlier
328 vibrissae [13, 14], and FST transgenic mice exhibited smaller hair follicles and rough and irregular
329 pelage [12]. Our previous study showed that sheep *FST* gene polymorphisms were associated with
330 wool quality traits [10]. Given these previous reports and our previous and present results, we
331 hypothesize that STAT3 may control sheep hair follicle development and wool trait formation at
332 least in part via directly regulating *FST* expression. To understand the molecular mechanisms
333 underlying hair follicle development and wool trait formation and to improve the quality of wool
334 in sheep, it is worth testing this hypothesis *in vivo* in the future.

Conclusion

In summary, in the present study, we closed the gap upstream of sheep genomic *FST* gene and demonstrated that STAT3 inhibits the proliferation of SFFs and HaCaT cells, at least in part via directly downregulating *FST* gene expression. Our findings will contribute to an understanding of the *FST* transcriptional regulation and the molecular mechanisms underlying hair follicle development and wool trait formation.

Figure legend

Fig. 1 Effects of STAT3 overexpression on *FST* gene promoter activity

(**A**) Conservation analysis of STAT3 binding sites in *FST* promoter among various species, STAT3 binding sites are indicated by capital letters and their locations are relative to the first nucleotide (A, +1) of the initiation codon (ATG) of *FST* gene. **(B)** Western blot identification of the STAT3 expression vector (pCMV-Myc-STAT3). Lane 1: the lysate of the cells transfected with pCMV-Myc-STAT3 (89 kDa); M: Protein markers (25 kDa-90 kDa). **(C)** The effects of mutation of the putative conserved STAT3 binding site on *FST* promoter activity. Either *FST* promoter pFST(-980/-340), pFST(-340/-980), or pFST(-980/-340)-mutSTAT3, along with pRL-TK, were co-transfected into HEK293 cells, and luciferase activity was measured at 48 h after transfection. Results were normalized with the Renilla luciferase activity and presented as fold inductions relative to the activity of cells that were transfected with pGL3-basic vector. **(D)** Effect of STAT3 on *FST* gene promoter activity. HEK293 cells were transiently co-transfected with either pFST(-980/-340) or pFST(-980/-340)-mutSTAT3 and pCMV-Myc-STAT3 or pCMV-Myc vector plus pRL-TK Renilla luciferase vector, subsequently, the HEK293 cells were lysed and luciferase activity was measured at 48 h after transfection. Results were normalized with the Renilla luciferase activity and presented as fold inductions relative to the activity of cells that were cotransfected with pFST(-980/-340) and pCMV-Myc-STAT3. **(E)** ChIP-qPCR analysis of the binding of STAT3 to the *FST* promoter. HEK293 cells were co-transfected with the pFST(-980/-340) and either pCMV-Myc-STAT3 or empty vector pCMV-Myc. At 48 h after transfection, ChIP was performed with a Myc-specific antibody or mouse IgG (negative control). Immunoprecipitated DNA was quantified by qRT-PCR using the specific pair of primers (Table 1), which was designed to amplify the -547/-356 region of the *FST* promoter.

Non-immunoprecipitated DNA (2%) was used as input DNA. Results were presented as fold enrichment over the negative control, which was prepared by the co-transfection of HEK293 cells with pFST(-980/-340) and pCMV-Myc-STAT3 and immunoprecipitated with mouse IgG. **(F)** The agarose gel electrophoresis analysis of ChIP-qPCR products. Lane 1: The qPCR products generated from the immunoprecipitated DNA which was isolated from the cells co-transfected with pCMV-Myc-STAT3 and pFST(-980/-340); Lane 2: The qPCR products generated from the immunoprecipitated DNA which was isolated from the cells co-transfected with pCMV-Myc and pFST(-980/-340). All data are representative of three independent experiments and are shown as the mean ± SEM. For each figure panel, different letters above error bars indicate a statistical significance ($P < 0.05$).

Fig. 2 Effects of *FST* overexpression on cell proliferation

(A) Western blot identification of the *FST* expression vector (pCMV-Myc-FST). Lane 1: the lysate of the cells transfected with pCMV-Myc-FST (38.2 kDa); Lane 2: positive control for Myc antibody (pCMV-Myc-POU2F3-3, 27.7 kDa). **(B and C)** Effect of *FST* overexpression on the proliferation of SFFs (**B**) and HaCaT cells (**C**). The SFFs and HaCaT cells were seeded in 96-well plates (5×10^4 cells / well) and transfected with pCMV-Myc-FST or empty vector pCMV-Myc (0.8 μg / well), and cell proliferation was assayed at indicated time points after transfection using CCK-8 kit. **(D and E)** Quantitative real-time PCR assay of *Ki67* (**D**) and *PCNA* (**E**) at 48 h of transfection in SFFs. The SFFs were seeded in 6-well plates (1.2×10^6 cells / well) and transfected with pCMV-Myc-FST or empty vector pCMV-Myc (4.0 μg / well). At 48 h post-transfection, total RNA was isolated from the SFFs with Trizol reagent, and gene expression was assessed using qRT-PCR. The gene expression was normalized to the housekeeping gene *GAPDH* using the $2^{-\Delta Ct}$ method, where $\Delta Ct = Ct_{[target\ gene]} — Ct_{[GAPDH]}$. Fold change was relative to the expression of the SFFs transfected with empty vector pCMV-Myc at 48 h. All data are representative of three independent experiments and are shown as the mean ± SEM. For each figure panel, statistical significance was indicated by $*P < 0.05$, $**P < 0.01$, and different letters above error bars indicate a statistical significance ($P < 0.05$).

Fig. 3 Effects of sheep STAT3 gene on cell proliferation and endogenous *FST* expression

(**A and B**) Effect of *STAT3* overexpression on the proliferation of SFFs **(A)** and HaCaT cells **(B)**. The SFFs and HaCaT cells were seeded in 96-well plates (5×10^4 cells / well) and transfected

with pCMV-Myc-STAT3 or empty vector pCMV-Myc (0.8 μg / well), and cell proliferation was assayed at indicated time points after transfection using CCK-8 kit. **(C - F)** Quantitative real-time PCR assay of *Ki67* **(C)**, *PCNA* **(D)**, and endogenous *FST* **(E** and **F)** expression at 48 h of transfection. The SFFs were seeded in 6-well plates (1.2×10^6 cells / well) and transfected with pCMV-Myc-STAT3 or empty vector pCMV-Myc (4.0 μg / well). At 48 h post-transfection, total RNA was isolated from the SFFs with Trizol reagent, and gene expression was assessed using qRT-PCR. The gene relative expression level was normalized to the housekeeping gene *GAPDH* using the $2^{-\Delta Ct}$ method, where $\Delta Ct=Ct_{[target\ gene]}—Ct_{[GAPDH]}$. Fold change was relative to the expression of the cells transfected with empty vector pCMV-Myc at 48 h. All data are representative of three independent experiments and are shown as the mean ± SEM. For each figure panel, statistical significance was indicated by $*P < 0.05$, $**P < 0.01$, and different letters above error bars indicate a statistical significance ($P < 0.05$).

Supplement fig. 1 Determination of the genomic gap upstream of sheep *FST* gene by genome walking PCR

The FST-SP1, FST-SP2, and FST-SP3 were designed according to the published sequences (GCF_002742125.1) on the NCBI website, and ZFP2, ZSP1 and ZSP2 were provided by KX Genome Walking Kit (Zoman Biotechnology, China). The primers pairs ZFP2/FST-SP1, ZSP1/FST-SP2 and ZSP2/FST-P3 were used to conduct the first-, second-and third-round PCRs for closing the genomic gap upstream of sheep *FST* gene according to the manufacturer's directions (more detailed information was shown in **Materials and Methods**).

Additional file

Supplement Table 1 Original data

Abbreviations

FST: follistain; STAT3: signal transducer and activator of transcription 3; SFFs: sheep fetal fibroblasts; HaCaT: human keratinocyte; ORS: outer root sheaths; IRS: inner root sheaths; FGF: fibroblast growth factor; TNF: tumor necrosis factor; TGF-β: transforming growth factor-β; Nrf2: nuclear factor erythroid 2-related factor 2; ERRβ: oestrogen-related receptor-β; CREB: cAMP responsive element binding protein; Smad3: SMAD family member 3; SP1: Sp1 transcription factor; TCF4: transcription factor 4; HOXA4: homeobox A4; E2F2: E2F transcription factor 2; HNF4: hepatocyte nuclear factor 4; FOXL2: forkhead box L2; IL-7A: interleukin 7A; IRF-4:

interferon regulatory factor 4; ATF3: activating transcription factor 3; PR: progesterone receptor; PI3K/Akt/mTOR: phosphatidylinositol-3-kinase/protein kinase B/mechanistic target of rapamycin kinase; GAPDH: glyceraldehyde 3-phosphate dehydrogenase; PCNA: proliferation cell nuclear antigen; TSS: transcription start site; CDS: coding regions; DMEM: Dulbecco's Modified Eagle's Medium; FBS: fetal bovine serum; SDS: sodium dodecyl sulfate; PBS: phosphate buffer saline; CCK-8: cell counting kit-8; ChIP: chromatin immunoprecipitation; qRT-PCR: quantitative reverse transcription-polymerase chain reaction;

Acknowledgments

This work was supported by Domain-Specific projects for transgenic biological breeding (2009ZX08009-160B and 2014ZX08009-002).

Availability of data and materials

The datasets during and/or analyzed during the current study available from the corresponding authors on reasonable request.

Authors' contributions

NW designed the study and provided funding support. HDX and GWM carried out the experiments, analyzed data and wrote the first draft of the manuscript. FM and BLN contributed to the subject discussion. HL and NW critically revised the manuscript. All authors reviewed and approved the final version of the manuscript.

All authors have read and approved the final manuscript.

Competing interests

The authors declare that they have no competing interests.

Ethics approval

The care and experimental use of sheep were approved by the Ministry of Science and Technology of the People's Republic of China (Approval number: 2006-398) and approved by the Laboratory Animal Management Committee of Northeast Agricultural University.

References

[1] Schneider M R, Schmidt-Ullrich R, Paus R. The hair follicle as a dynamic miniorgan. Curr Biol. 2009; 19: R132-42.

[2] Plowman J E, Harland D P. The follicle cycle in brief. Adv Exp Med Biol. 2018; 1054: 15-7.

[3] Alonso L, Fuchs E. The hair cycle. J Cell Sci. 2006; 119: 391-3.

[4] Stenn K S, Paus R. Controls of hair follicle cycling. Physiol Rev. 2001; 81: 449-94.

[5] Wang X S, Tredget E E, Wu Y. Dynamic signals for hair follicle development and regeneration. Stem Cells Dev. 2012; 21: 7-18.
[6] Müller-Röver S, Handjiski B, Van Der Veen C, Eichmüller S, Foitzik K, Mckay I A, et al. A comprehensive guide for the accurate classification of murine hair follicles in distinct hair cycle stages. J Invest Dermatol. 2001; 117: 3-15.
[7] Pispa J, Thesleff I. Mechanisms of ectodermal organogenesis. Dev Biol. 2003; 262: 195-205.
[8] Liu J J, Xu Y X, Wu Q F, Ding Q, Fan W X. Sirtuin-1 protects hair follicle stem cells from TNFα-mediated inflammatory stress via activating the MAPK-ERK-Mfn2 pathway. Life Sci. 2018; 212: 213-24.
[9] Li Z, Ryu S W, Lee J, Choi K, Kim S, Choi C. Protopanaxatirol type ginsenoside Re promotes cyclic growth of hair follicles via inhibiting transforming growth factor β signaling cascades. Biochem Biophys Res Commun. 2016; 470: 924-9.
[10] Ma G W, Chu Y K, Zhang W J, Qin F Y, Xu S S, Yang H, et al. Polymorphisms of *FST* gene and their association with wool quality traits in Chinese Merino sheep. Plos One. 2017; 12: e0174868.
[11] Guo Q X, Kumar T R, Woodruff T, Hadsell L A, Demayo F J, Matzuk M M. Overexpression of mouse follistatin causes reproductive defects in transgenic mice. Mol Endocrinol. 1998; 12: 96-106.
[12] Wankell M, Munz B, Hübner G, Hans W, Wolf E, Goppelt A, et al. Impaired wound healing in transgenic mice overexpressing the activin antagonist follistatin in the epidermis. EMBO J. 2001; 20: 5361-72.
[13] Nakamura M, Matzuk M M, Gerstmayer B, Bosio A, Lauster R, Miyachi Y, et al. Control of pelage hair follicle development and cycling by complex interactions between follistatin and activin. FASEB J. 2003; 17: 497-9.
[14] Matzuk M M, Lu N, Vogel H, Sellheyer K, Roop D R, Bradley A. Multiple defects and perinatal death in mice deficient in follistatin. Nature. 1995; 374: 360-3.
[15] Jhaveri S, Erzurumlu R S, Chiaia N, Kumar T R, Matzuk M M. Defective whisker follicles and altered brainstem patterns in activin and follistatin knockout mice. Mol Cell Neurosci. 1998; 12: 206-19.
[16] Lin C, Zhao X Y, Sun D, Zhang L D, Fang W P, Zhu T J, et al. Transcriptional activation of follistatin by Nrf2 protects pulmonary epithelial cells against silica nanoparticle-induced oxidative stress. Sci Rep. 2016; 6: 21133.
[17] Han X H, Jin Y R, Tan L, Kosciuk T, Lee J S, Yoon J K. Regulation of the follistatin gene by RSPO-LGR4 signaling via activation of the WNT/β-catenin pathway in skeletal myogenesis. Mol Cell Biol. 2014; 34: 752-64.
[18] Yang H J, Zhang Z H, Xue L Y. Structural characterization and functional analysis of the follistatin promoter of *Larimichthys crocea*. DNA Cell Biol. 2016; 35: 471-9.
[19] Jones A E, Price F D, Le Grand F, Soleimani V D, Dick S A, Megeney L A, et al. Wnt/β-catenin controls follistatin signalling to regulate satellite cell myogenic potential. Skelet Muscle. 2015; 5: 14.
[20] Sengupta D, Bhargava D K, Dixit A, Sahoo B S, Biswas S, Biswas G, et al. ERR-*β*signalling through FST and BCAS2 inhibits cellular proliferation in breast cancer cells. Br J Cancer. 2014; 110: 2144-58.

[21] Necela B M, Su W D, Thompson E A. Peroxisome proliferator-activated receptor gamma down-regulates follistatin in intestinal epithelial cells through SP1. J Biol Chem. 2008; 283: 29784-94.
[22] Mehta N, Zhang D, Li R Z, Wang T, Gava A, Parthasarathy P, et al. Caveolin-1 regulation of Sp1 controls production of the antifibrotic protein follistatin in kidney mesangial cells. Cell Commun Signal. 2019; 17: 37.
[23] Sano S, Chan K S, Digiovanni J. Impact of STAT3 activation upon skin biology: a dichotomy of its role between homeostasis and diseases. J Dermatol Sci. 2008; 50: 1-14.
[24] Rao D, Macias E, Carbajal S, Kiguchi K, Digiovanni J. Constitutive Stat3 activation alters behavior of hair follicle stem and progenitor cell populations. Mol Carcinog. 2015; 54: 121-33.
[25] Shibata A, Tanahashi K, Sugiura K, Akiyama M. TRPS1 haploinsufficiency results in increased STAT3 and SOX9 mRNA expression in hair follicles in trichorhinophalangeal syndrome. Acta Derm venereol. 2015; 95: 620-1.
[26] Nelson A M, Katseff A S, Resnik S R, Garza L A. Interleukin 6 promotes adult de novo hair follicle organogenesis through STAT3 phosphorylation. J Investig Dermatol Symp Proc. 2013; 133: 1428.
[27] Green M R, Sambrook J. Molecular Cloning: A laboratory manual (4 th ed). New York: Cold Spring Harbor Laboratory Press, 2014.
[28] Shapter F M, Waters D L E. Genome walking. Methods Mol Biol. 2014; 1099: 133-46.
[29] Ovcharenko I, Loots G G, Giardine B M, Hou M M, Ma J, Hardison R C, et al. Mulan: multiple-sequence local alignment and visualization for studying function and evolution. Genome Res. 2005; 15: 184-94.
[30] Deng X, Zhang W W, O-Sullivan I, Williams J B, Dong Q M, Park E A, et al. FoxO1 inhibits sterol regulatory element-binding protein-1c (SREBP-1c) gene expression via transcription factors Sp1 and SREBP-1c. J Biol Chem. 2012; 287: 20132-43.
[31] Tatler A L, Habgood A, Porte J, John A E, Stavrou A, Hodge E, et al. Reduced ets domain-containing protein Elk1 promotes pulmonary fibrosis via increased integrin αvβ6 expression. J Biol Chem. 2016; 291: 9540-53.
[32] Asp P. How to combine ChIP with qPCR. Methods Mol Biol. 2018; 1689: 29-42.
[33] Yu H, Lee H, Herrmann A, Buettner R, Jove R. Revisiting STAT3 signalling in cancer: new and unexpected biological functions. Nat Rev Cancer. 2014; 14: 736-46.
[34] Sano S, Itami S, Takeda K, Tarutani M, Yamaguchi Y, Miura H, et al. Keratinocyte-specific ablation of Stat3 exhibits impaired skin remodeling, but does not affect skin morphogenesis. EMBO J. 1999; 18: 4657-68.
[35] Sano S, Kira M, Takagi S, Yoshikawa K, Takeda J, Itami S. Two distinct signaling pathways in hair cycle induction: Stat3-dependent and -independent pathways. Proc Nat Acad Sci U S A. 2000; 97: 13824-9.
[36] Gilson H, Schakman O, Kalista S, Lause P, Tsuchida K, Thissen J P. Follistatin induces muscle hypertrophy through satellite cell proliferation and inhibition of both myostatin and activin. Am J Physiol Endocrinol Metab. 2009; 297: E157-64.
[37] Liu H H, Wang J W, Yu H Y, Zhang R P, Chen X, Jin H B, et al. Injection of duck recombinant follistatin fusion protein into duck muscle tissues stimulates satellite cell proliferation and muscle fiber hypertrophy. Appl Microbiol Biotechnol. 2012; 94: 1255-63.

[38] Lee C K, Raz R, Gimeno R, Gertner R, Wistinghausen B, Takeshita K, et al. STAT3 is a negative regulator of granulopoiesis but is not required for G-CSF-dependent differentiation. Immunity. 2002; 17: 63-72.
[39] Matsui T, Kinoshita T, Hirano T, Yokota T, Miyajima A. STAT3 down-regulates the expression of cyclin D during liver development. J Biol Chem. 2002; 277: 36167-73.
[40] Suemoto H, Muragaki Y, Nishioka K, Stao M, Ooshima A, Itoh S, et al. TRPS1 regualtes proliferation and apotosis of chondrocytes through STAT3 signaling. Dev Biol. 2007; 312: 572-81.
[41] Han Y Y, Wang T X, Sun S D, Zhai Z H, Tang S J. Cloning of the promoter region of a human gene, FOXL2, and its regulation by STAT3. Mol Med Rep. 2017; 16: 2856-62.
[42] Kunkl M, Mastrogiovanni M, Porciello N, Caristi S, Monteleone E, Arcieri S, et al. CD28 individual signaling up-regulates human IL-17A expression by promoting the recruitment of RelA/NF-κB and STAT3 transcription factors on the proximal promoter. Front Immunol. 2019; 10: 864.
[43] Chen W, Nyuydzefe M S, Weiss J M, Zhang J Y, Waksal S D, Zanin-Zhorov A. ROCK2, but not ROCK1 interacts with phosphorylated STAT3 and co-occupies TH17/TFH gene promoters in TH17-activated human T cells. Sci Rep. 2019; 8: 16636.
[44] Kong D G, Li A P, Liu Y, Cui Q X, Wang K, Zhang D, et al. SIX1 activates STAT3 signaling to promote the proliferation of thyroid carcinoma via EYA1. Front Oncol. 2019; 9: 1450.
[45] Li X X, Liu H H, Wang H H, Sun L L, Ding F, Sun W Q, et al. Follistatin could promote the proliferation of duck primary myoblasts by activating PI3K/Akt/mTOR signalling. Biosci Rep. 2014; 34: e00143.
[46] Karve T M, Anju P, Sneed R, Salamanca C, Li X, Xu J W, et al. BRCA1 regulates follistatin function in ovarian cancer and human ovarian surface epithelial cells. Plos One. 2012; 7: e37697.
[47] Bromberg J F, Wrzeszczynska M H, Devgan G, Zhao Y X, Pestell R G, Albanese C, et al. Stat3 as an oncogene. Cell. 1999; 98: 295-303.
[48] Ma J H, Qin L, Li X. Role of STAT3 signaling pathway in breast cancer. Cell Commun Signal. 2020; 18: 33.
[49] Martin P. Wound healing--aiming for perfect skin regeneration. Science. 1997; 276: 75-81.
[50] Haniffa M A, Collin M P, Buckley C D, Dazzi F. Mesenchymal stem cells: the fibroblasts'new clothes? Haematologica. 2009; 94: 258-63.
[51] Wilson V G. Growth and differentiation of HaCaT keratinocytes. Methods Mol Biol. 2014; 1195: 33-41.
[52] Deyrieux A F, Wilson V G. In vitro culture conditions to study keratinocyte differentiation using the HaCaT cell line. Cytotechnology. 2007; 54: 77-83.
[53] Mcdowall M, Edwards N M, Jahoda C A B, Hynd P I. The role of activins and follistatins in skin and hair follicle development and function. Cytokine Growth Factor Rev. 2008; 19: 415-26.

Figures

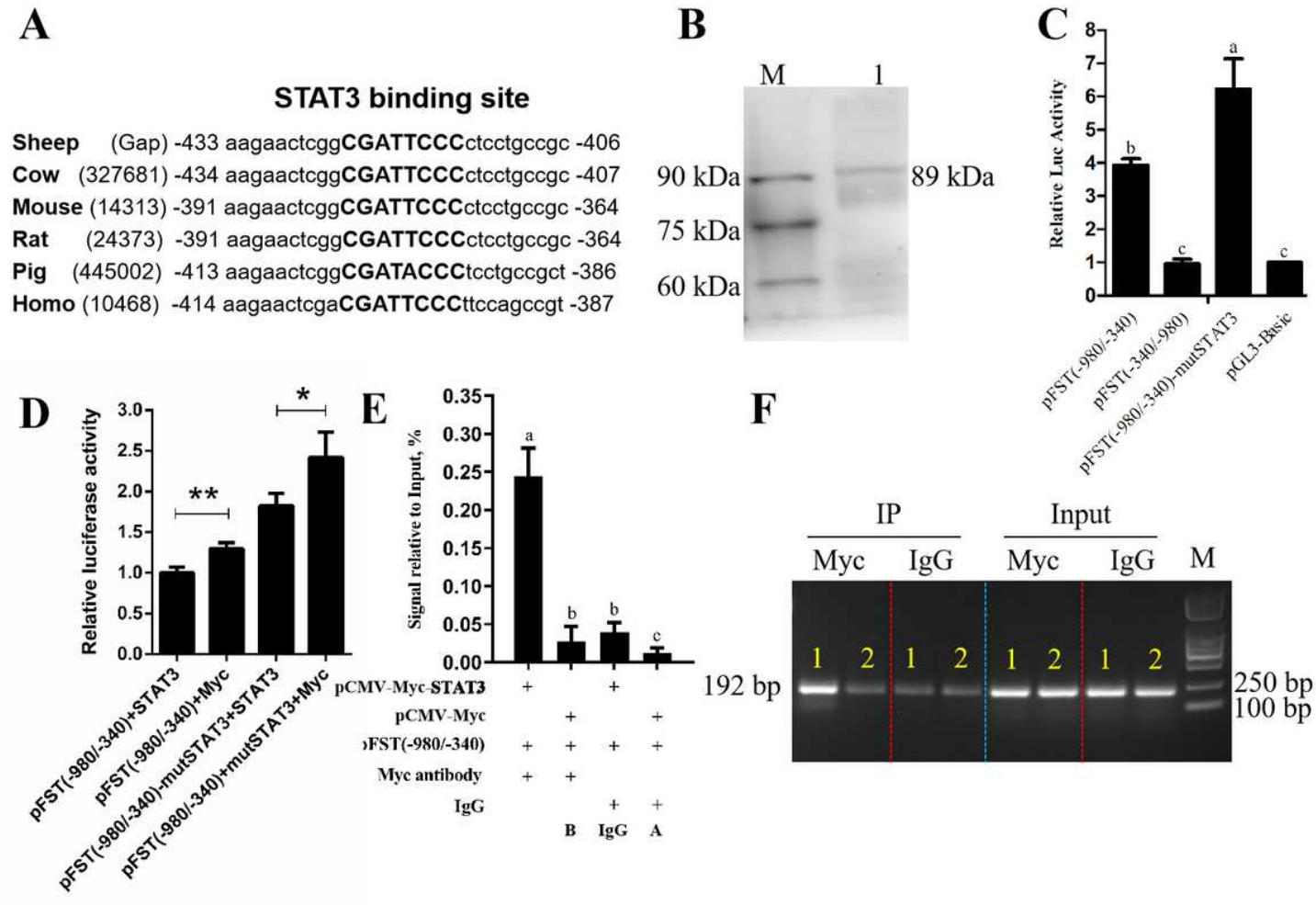

Figure 1

Effects of STAT3 overexpression on FST gene promoter activity (A) Conservation analysis of STAT3 binding sites in FST promoter among various species, STAT3 binding sites are indicated by capital letters and their locations are relative to the first nucleotide (A, +1) of the initiation codon (ATG) of FST gene. (B) Western blot identification of the STAT3 expression vector (pCMV-Myc-STAT3). Lane 1: the lysate of the cells transfected with pCMV-Myc-STAT3 (89 kDa); M: Protein markers (25 kDa-90 kDa). (C) The effects of mutation of the putative conserved STAT3 binding site on FST promoter activity. Either FST promoter pFST(-980/-340), pFST(-340/-980), or pFST(-980/-340)-mutSTAT3, along with pRL-TK, were co-transfected into HEK293 cells, and luciferase activity was measured at 48 h after transfection. Results were normalized with the Renilla luciferase activity and presented as fold inductions relative to the activity of cells that were transfected with pGL3-basic vector. (D) Effect of STAT3 on FST gene promoter activity. HEK293 cells were transiently co-transfected with either pFST(-980/-340) or pFST(-980/-340)-mutSTAT3 and pCMV-Myc-STAT3 or pCMV-Myc vector plus pRL-TK Renilla luciferase vector, subsequently, the HEK293 cells were lysed and luciferase activity was measured at 48 h after transfection. Results were normalized with the Renilla luciferase activity and presented as fold inductions

relative to the activity of cells that were cotransfected with pFST(-980/-340) and pCMV-Myc-STAT3. (E) ChIP-qPCR analysis of the binding of STAT3 to the FST promoter. HEK293 cells were co-transfected with the pFST(-980/-340) and either pCMV-Myc-STAT3 or empty vector pCMV-Myc. At 48 h after transfection, ChIP was performed with a Myc-specific antibody or mouse IgG (negative control). Immunoprecipitated DNA was quantified by qRT-PCR using the specific pair of primers (Table 1), which was designed to amplify the -547/-356 region of the FST promoter. Non-immunoprecipitated DNA (2%) was used as input DNA. Results were presented as fold enrichment over the negative control, which was prepared by the co-transfection of HEK293 cells with pFST(-980/-340) and pCMV-Myc-STAT3 and immunoprecipitated with mouse IgG. (F) The agarose gel electrophoresis analysis of ChIP-qPCR products. Lane 1: The qPCR products generated from the immunoprecipitated DNA which was isolated from the cells co-transfected with pCMV-Myc-STAT3 and pFST(-980/-340); Lane 2: The qPCR products generated from the immunoprecipitated DNA which was isolated from the cells co-transfected with pCMV-Myc and pFST(-980/-340). All data are representative of three independent experiments and are shown as the mean ± SEM. For each figure panel, different letters above error bars indicate a statistical significance ($P < 0.05$).

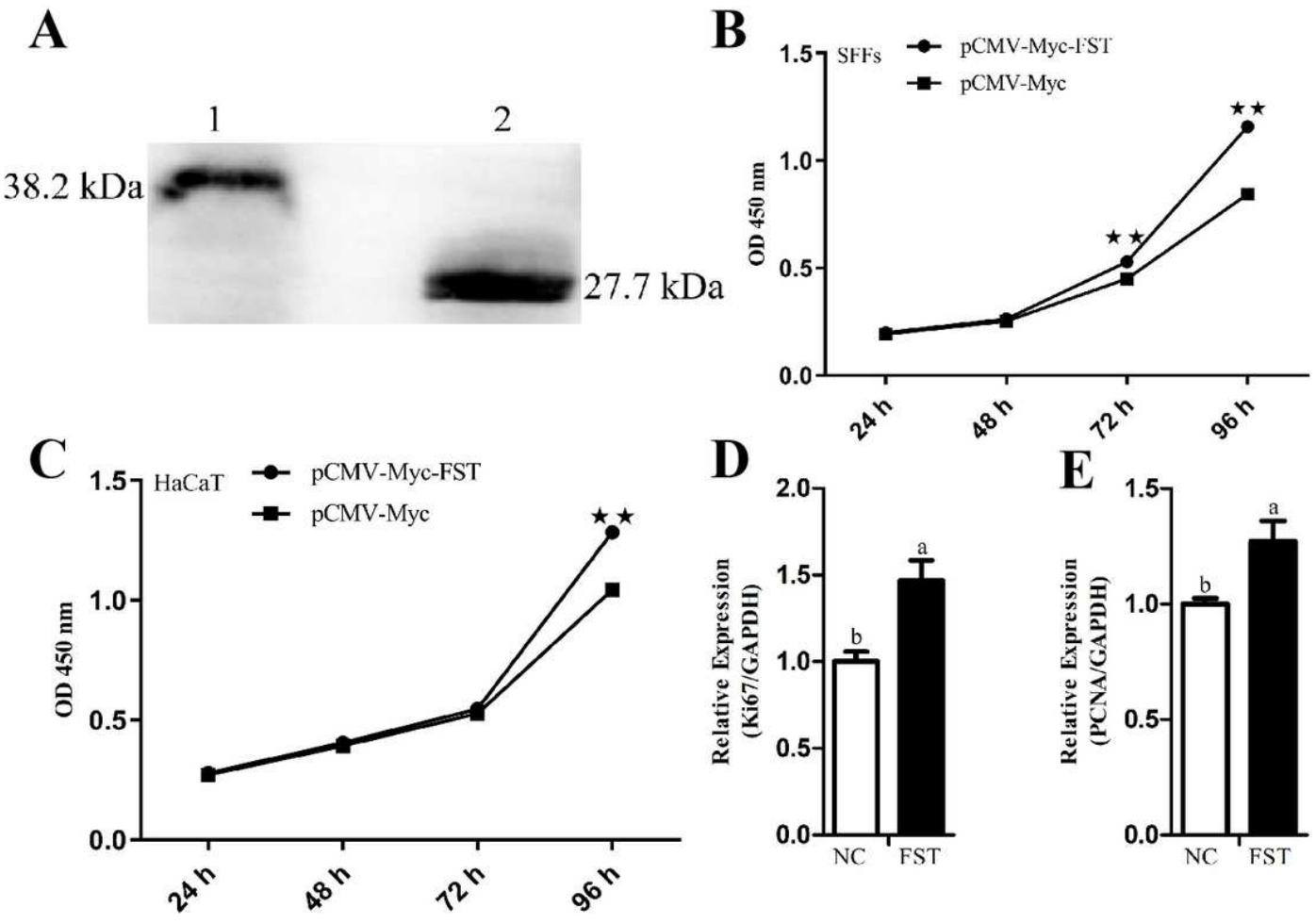

Figure 2

Effects of FST overexpression on cell proliferation (A) Western blot identification of the FST expression vector (pCMV-Myc-FST). Lane 1: the lysate of the cells transfected with pCMV-Myc-FST (38.2 kDa); Lane 2: positive control for Myc antibody (pCMV-Myc-POU2F3-3, 27.7 kDa). (B and C) Effect of FST overexpression on the proliferation of SFFs (B) and HaCaT cells (C). The SFFs and HaCaT cells were seeded in 96-well plates (5 × 104 cells / well) and transfected with pCMV-Myc-FST or empty vector pCMV-Myc (0.8 μg / well), and cell proliferation was assayed at indicated time points after transfection using CCK-8 kit. (D and E) Quantitative real-time PCR assay of Ki67 (D) and PCNA (E) at 48 h of transfection in SFFs. The SFFs were seeded in 6-well plates (1.2 × 106 cells / well) and transfected with pCMV-Myc-FST or empty vector pCMV-Myc (4.0 μg / well). At 48 h post-transfection, total RNA was isolated from the SFFs with Trizol reagent, and gene expression was assessed using qRT-PCR. The gene expression was normalized to the housekeeping gene GAPDH using the 2-ΔCt method, where ΔCt=Ct[target gene]—Ct[GAPDH]. Fold change was relative to the expression of the SFFs transfected with empty vector pCMV-Myc at 48 h. All data are representative of three independent experiments and are shown as the mean ± SEM. For each figure panel, statistical significance was indicated by *P < 0.05, **P < 0.01, and different letters above error bars indicate a statistical significance (P < 0.05).

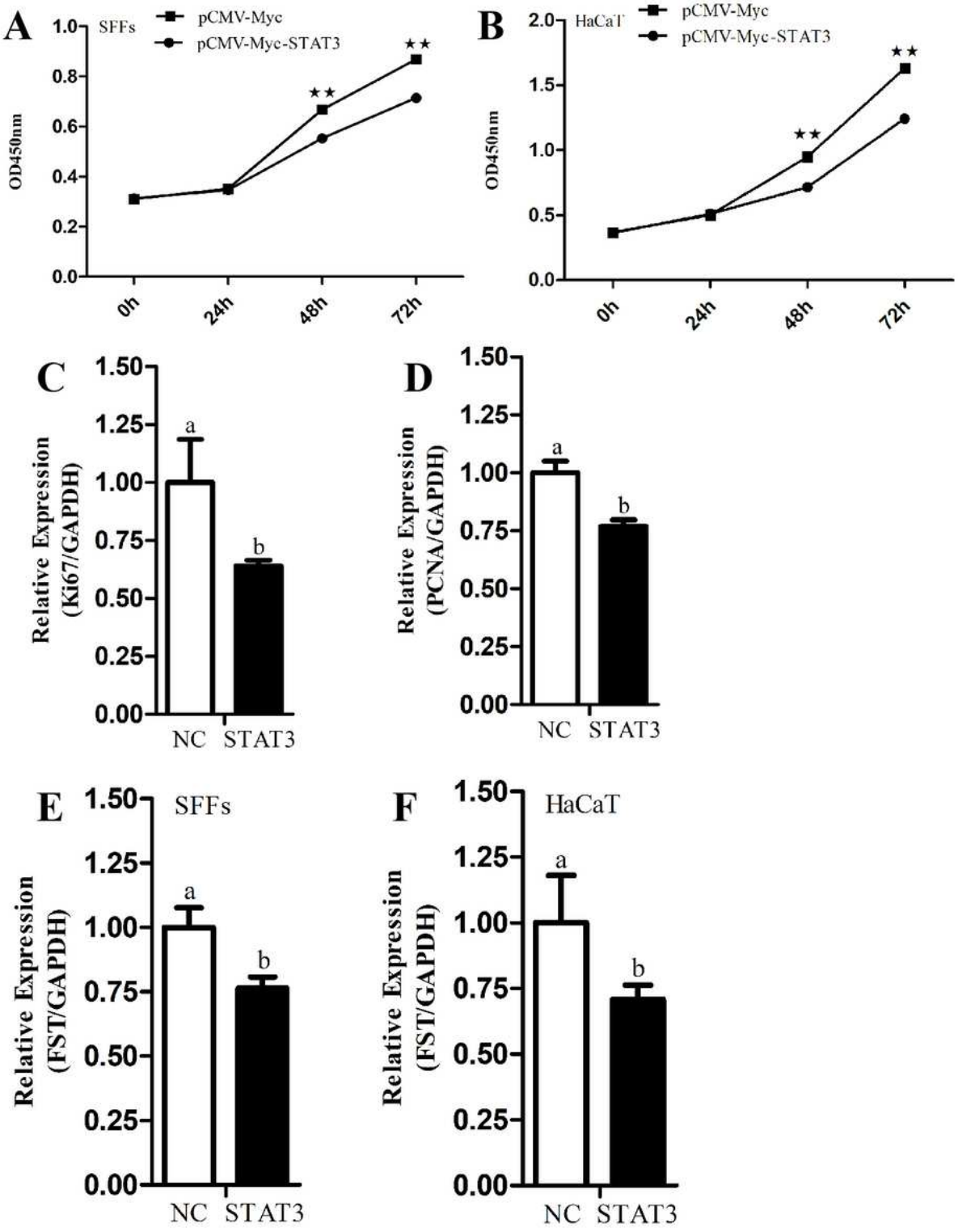

Figure 3

Effects of sheep STAT3 gene on cell proliferation and endogenous FST expression (A and B) Effect of STAT3 overexpression on the proliferation of SFFs (A) and HaCaT cells (B). The SFFs and HaCaT cells were seeded in 96-well plates (5 × 104 cells / well) and transfected with pCMV-Myc-STAT3 or empty vector pCMV-Myc (0.8 μg / well), and cell proliferation was assayed at indicated time points after transfection using CCK-8 kit. (C - F) Quantitative real-time PCR assay of Ki67 (C), PCNA (D), and

endogenous FST (E and F) expression at 48 h of transfection. The SFFs were seeded in 6-well plates (1.2 × 106 cells / well) and transfected with pCMV-Myc-STAT3 or empty vector pCMV-Myc (4.0 μg / well). At 48 h post-transfection, total RNA was isolated from the SFFs with Trizol reagent, and gene expression was assessed using qRT-PCR. The gene relative expression level was normalized to the housekeeping gene GAPDH using the 2-ΔCt method, where ΔCt=Ct[target gene]—Ct[GAPDH]. Fold change was relative to the expression of the cells transfected with empty vector pCMV-Myc at 48 h. All data are representative of three independent experiments and are shown as the mean ± SEM. For each figure panel, statistical significance was indicated by *P < 0.05, **P < 0.01, and different letters above error bars indicate a statistical significance (P < 0.05).

Supplementary Files

This is a list of supplementary files associated with this preprint. Click to download.

- Supplementfigure1.tif
- Supplementtable.xls